Available online at www.sciencedirect.com
SCIENCE DIRECT®
Journal of Catalysis 220 (2003) 500–512
JOURNAL OF CATALYSIS
www.elsevier.com/locate/jcat

An operando optical fiber UV–vis spectroscopic study of the catalytic decomposition of NO and N_2O over Cu-ZSM-5

Marijke H. Groothaert, Kristof Lievens, Hugo Leeman, Bert M. Weckhuysen, and Robert A. Schoonheydt *

Center for Surface Chemistry and Catalysis, K.U. Leuven, Kasteelpark Arenberg 23, B-3001 Leuven, Belgium

Received 16 April 2003; revised 12 August 2003; accepted 12 August 2003

Abstract

The role of the bis(μ-oxo)dicopper core, i.e., $[Cu_2(\mu\text{-}O)_2]^{2+}$, in the decomposition of NO and N_2O by the Cu-ZSM-5 zeolite has been studied with combined operando UV–vis monitoring of the catalyst and on-line GC analysis. An optical fiber was mounted on the outer surface of the quartz wall of the plug-flow reactor and collected the UV–vis diffuse reflectance spectra under true catalytic conditions. Measurement under transient reaction conditions indicated that $[Cu_2(\mu\text{-}O)_2]^{2+}$ is formed by O abstraction of N_2O, which is an intermediate in the NO decomposition. This conversion of N_2O to N_2 and O_2 is strongly retarded below 673 K. Above 673 K, the produced $[Cu_2(\mu\text{-}O)_2]^{2+}$ fulfills the role of O_2 release, guaranteeing the self-reduction of the catalytic site. Studying the NO decomposition as a function of the O_2 content in the feed strongly suggested that O_2 release from $[Cu_2(\mu\text{-}O)_2]^{2+}$ is rate limiting in the NO decomposition at 773 K.

Keywords: Cu-ZSM-5; bis(μ-oxo)dicopper; NO decomposition; N_2O decomposition; UV–vis spectroscopy; Operando spectroscopy

1. Introduction

A very appealing method for the removal of NO is its direct decomposition into molecular N_2 and O_2. The decomposition of NO is thermodynamically favored at temperatures below 1000 K [1]; e.g., at room temperature the Gibbs free energy of reaction amounts to -175 kJ mol^{-1} [2,3]. However, the reaction is kinetically retarded due to the very high activation energy of about 300 kJ mol^{-1} [4]. A whole series of catalysts was explored over the last 50 years, but no appreciable reaction rates were obtained till the epoch-making finding of Iwamoto et al. in 1986 [5]. They reported the uniquely high and stable activity of overexchanged Cu-ZSM-5 for the direct NO decomposition [5]. However, tests under conditions representative of automotive exhaust gases pointed toward two important limitations of Cu-ZSM-5 for a practical application: (1) a too low activity by 1–2 orders of magnitude and (2) the suppression of the activity by water vapor and SO_2 [1]. Recently, much research has been done on modifications of Cu-ZSM-5, e.g., by adding a second cation or altering the support [6–10], in order to increase the activity and stability. Other catalysts that are active for NO decomposition include Co_3O_4 modified with Ag and Na [11], perovskite-type compounds [12], Cu/Mg/Al oxides derived from hydrotalcites [13], and BaO supported on MgO [14], but none of these materials displays the level of activity required for practical application. All of the active catalysts have a common feature in that they are able to release oxygen at moderate temperatures [14]. Cu-ZSM-5 also displays high and stable activity for the decomposition of N_2O to N_2 and O_2 [15–17]. Although a number of metal oxides are known to decompose N_2O to its elements at elevated temperatures [18], Cu- or Co-exchanged Beta, ZSM-5, or mordenite zeolites supported on a ceramic honeycomb are envisaged as promising catalysts [19,20].

Much research has been dedicated to the identification of the active sites in Cu-ZSM-5 and the NO decomposition reaction mechanism. A 100% selective conversion of NO into N_2 and O_2 can be achieved over Cu-ZSM-5 above 623 K with maximum activity in the temperature range 723–773 K [21]. Several explanations for this profile have been proposed, such as (1) the desorption of oxygen [21], (2) the instability or surface nitrates [22], and (3) the adsorption equilibrium of NO [23]. Li and Hall [24] suggested that

* Corresponding author.
E-mail address: robert.schoonheydt@agr.kuleuven.ac.be (R.A. Schoonheydt).

0021-9517/$ – see front matter
doi:10.1016/j.jcat.2003.08.009

the NO_2 production observed in case of incomplete NO decomposition results from the reaction of NO with produced O_2 in the cool exit zone of the reactor. It is known that the equilibrium-controlled reaction ($2NO + O_2 \leftrightarrow 2NO_2$) favors NO_2 formation at room temperature; however, this reaction does not proceed far to the right at elevated temperatures (K (298 K) $= 2.4 \times 10^{12}$ atm^{-1}; K (773 K) $=$ 0.82 atm^{-1}) [24].

In the earliest NO decomposition schemes, Cu^{2+} [25] or Cu^{2+}–O^- [26] were put forward as catalytic centers without invoking a cyclic redox process. Now, a growing consensus is found that monovalent copper participates in the NO decomposition reaction [27–33]. A number of experimental and computational studies propose a redox process cycling between Cu(I) and Cu(II)–ELO species (ELO, extralattice oxygen) [27–30,33–38]. However, the identity of the ELO is not clear. Some studies [27–30] have suggested that the ELO is associated with mononuclear copper and is of the structure Cu^{2+}–O^- or Cu^{2+}–O^{2-}. Alternatively, others [21,22, 33,39–41] proposed that a single-O-bridged copper pair, i.e., $[CuOCu]^{2+}$, is essential in the NO decomposition cycle. Recent computational contributions of Goodman et al. [38,42] stressed the eventual role of double-O-bridged copper pairs, i.e., $[CuO_2Cu]^{2+}$. Based on this knowledge, $[CuO_2Cu]^{2+}$ has been included in some recent NO decomposition cycles [43–45] and is proposed to play a role in O_2 formation, either directly via the release of O_2 or indirectly via recombinative desorption requiring vicinal oxocations or NO-mediated oxygen removal. However, in the latter studies, none of the double-O-bridged copper pairs that are proposed in the theoretical contribution of Goodman et al. [38] were identified spectroscopically.

In a recent EPR (electron paramagnetic resonance) study of our group [46], we found that calcined Cu-ZSM-5 samples with Cu/Al $>$ 0.2 are characterized by a fraction of EPR-undetectable copper, which grows with increasing Cu/Al ratio. This EPR silent copper fraction took our attention since the NO decomposition activity has a S-shaped dependence on the copper exchange level in ZSM-5 [15, 21,23]. The NO decomposition rate gradually increases for the lower exchange levels and increases sharply above the Cu/Al ratio of 0.2 [23]. Therefore, we applied XAFS and UV–vis–NIR spectroscopy to identify the large fraction of EPR silent copper (81% of the total Cu content) in the calcined overexchanged Cu-ZSM-5 (Cu/Al $= 0.6$). EXAFS pointed to a Cu$\cdots$Cu contribution at 2.87 Å with a coordination number of 1. The corresponding UV–vis–NIR spectrum is characterized by an intense CT (charge transfer) band at 22,700 cm^{-1} and a weak CT band at 30,000 cm^{-1}. For the first time, these combined EPR, XAFS, and UV–vis–NIR data were compared with the large databank of well-characterized copper centers in enzymes and synthetic model complexes and led to the identification of the bis(μ-oxo)dicopper core, i.e., $[Cu_2(\mu\text{-}O)_2]^{2+}$ (Structure A) in calcined overexchanged Cu-ZSM-5 [47–49]. We showed that the catalytic NO decomposition activity and the presence of the bis(μ-oxo)dicopper core occur concomitantly, strongly suggesting a correlation [49]. Further, the in situ XAFS data of the latter study [49] are consistent with the formation of a large fraction of this double-O-bridged Cu pair during NO decomposition.

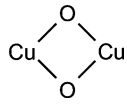

Structure A.

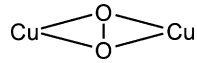

Structure B.

So far, the bis(μ-oxo)dicopper core had only been identified in synthetic model complexes in solution [50]. In this homogeneous chemistry, the bis(μ-oxo)dicopper core is capable of isomerizing to the (μ-η^2:η^2-peroxo)dicopper core, i.e., $[Cu_2(\mu\text{-}\eta^2\text{:}\eta^2\text{-}O_2)]^{2+}$ (Structure B) [51,52]. The latter peroxo-dicopper core is also present in the enzyme hemocyanin, found in arthropods and mollusks, where it performs the reversible binding of O_2 [53,54]. Therefore, we suggested that the bis(μ-oxo)dicopper core in Cu-ZSM-5 fulfills the key role of the continuous O_2 release and in this way guarantees the sustained high activity of Cu-ZSM-5 [49].

In the present contribution, an operando UV–vis diffuse reflectance spectroscopic study of Cu-ZSM-5 during the decomposition of NO and N_2O is presented. So far, this technique has not been applied in the research on Cu-ZSM-5. Optical fiber technology is implemented in the setup as this equipment is highly compatible with a plug-flow reactor and the elevated temperatures [55]. The use of a photodiode array detector guarantees a simultaneous detection of the full wavelength region of the spectrum. This operando UV–vis spectroscopy in combination with on-line GC analysis allows a direct study of the role of the bis(μ-oxo)dicopper core in the catalytic NO and N_2O decomposition cycles.

2. Experimental section

2.1. Samples

K-ZSM-5 (Si/Al $= 31$, ExxonMobil Chemical) was put in the Na^+ form and overexchanged with Cu^{2+} according to the method of Iwamoto et al. [56]. One gram of Na-ZSM-5 was ion-exchanged in 25 ml of a 0.01 M $Cu(CH_3CO_2)_2 \cdot H_2O$ solution at ambient temperature for 24 h. This procedure was repeated three times. Then the sample was washed and dried at 383 K. The Cu and Al contents were determined by inductively coupled plasma (ICP), resulting in a Cu/Al ratio of 0.58.

A series of Cu-ZSM-5 samples with increasing Cu loading was prepared starting from Na-ZSM-5 (Si/Al $= 12$, ALSI-PENTA). Four samples were prepared by adding 1 g Na-ZSM-5 to 250 ml of a 0.0005, 0.001, 0.0015, and 0.002 M $Cu(CH_3CO_2)_2 \cdot H_2O$ solution respectively. After 24 h of ion exchange at ambient temperature, the samples

Table 1
Summary of the treatments of the Cu-ZSM-5 samples

Experiment (sample)	Temperature	Feed
Calcination (CZ-31-0.58)	2 K min^{-1} to 773 K and 2 h at final temperature	O_2 (50 ml min^{-1})
Standard pretreatment for catalytic testing	5 K min^{-1} to 773 K and 4 h at final temperature	He (50 ml min^{-1})
NO decomposition as function of T (CZ-31-0.58)	Equilibration (at least 2 h) until steady-state activity at each temperature: 773, 723, 673, 623, 573, 523 K	1 mol% NO in He (15 ml min^{-1})
NO decomposition as function of copper loading (CZ-12-0.10; CZ-12-0.22; CZ-12-0.31; CZ-12-0.38; CZ-12-0.54; CZ-12-0.58)	773 K	1 mol% NO in He (15 ml min^{-1}) 2 mol% NO in He (15 ml min^{-1}) 1 mol% NO in He (45 ml min^{-1}) 2 mol% NO in He (45 ml min^{-1}) (2 h of equilibration each time)
NO decomposition with O_2 in feed (CZ-31-0.58)	773 K	1 mol% NO with 0, 2, 4, 8, 16, 0 mol% O_2 (2 h of equilibration each time) in He (15 ml min^{-1})
N_2O decomposition as function of *T* (CZ-31-0.58)	Equilibration (at least 2 h) until steady-state activity at each temperature: 773, 723, 673, 623, 573, 523 K	1 mol% N_2O in He (15 ml min^{-1})
N_2O decomposition with O_2 in feed (CZ-31-0.58)	773 K	1, 2 or 3 mol% N_2O with 0, 2, 4, 8, 16, 0 mol% O_2 (2 h of equilibration each time) in He (15 ml min^{-1})
N_2O decomposition during temperature drop (CZ-31-0.58)	5 K min^{-1} from 723 to 673 K	1 mol% N_2O in He (15 ml min^{-1})
O_2 flow during temperature drop (CZ-31-0.58)	5 K min^{-1} from 723 to 673 K	2 mol% O_2 in He (15 ml min^{-1})

were washed and dried at 383 K. Two samples were prepared by adding 1 g Na-ZSM-5 to 63 ml of a 0.01 and 0.0125 M $Cu(CH_3CO_2)_2 \cdot H_2O$ solution, respectively. The latter ion-exchange procedure was repeated three times. Then the samples were washed and dried at 383 K. The Cu and Al contents were determined by ICP, resulting in Cu/Al ratios of 0.10, 0.22, 0.31, 0.38, 0.54, and 0.58.

The as-prepared Cu-ZSM-5 samples will be denoted as CZ–X–Y, where X gives the Si/Al ratio and Y the Cu/Al ratio. Prior to catalytic testing, the samples were calcined overnight (heating rate of 2 K min^{-1} to 723 K; O_2 flow of 50 ml min^{-1}).

2.2. Catalytic testing

The Cu-ZSM-5 material was tested for the decomposition of NO and N_2O in a plug-flow reactor (i.d. = 8 mm). The amount of 0.5 g of the sample (pellets of 0.25–0.4 mm) was loaded in the reactor. The standard pretreatment consisted of a preheating at 5 K min^{-1} to 773 K (4 h) under a He flow (50 ml min^{-1}). The details of the subsequent treatments are summarized in Table 1. The reaction feed was obtained by blending 10 mol% NO in He, 5 mol% N_2O in He, 100 mol% O_2, and balance He. The resulting inlet for the different experiments is summarized in Table 1. Table 1 also indicates that the overall flow amounted to 15 or 45 ml min^{-1} in each experiment. Based on an apparent zeolite density of 0.5 g cm^{-3}, the calculated gas hourly space velocity (GHSV) was 900 h^{-1} ($W/F = 2.0$ g s cm^{-3}) or 2700 h^{-1} ($W/F = 0.67$ g s cm^{-3}), respectively. A HP 4890D gas chromatograph (GC) equipped with a packed column (13X) and a TCD detector was used to monitor on line the concentration of N_2, O_2, and N_2O in the effluent.

2.3. Operando UV–vis spectroscopy

The term "operando spectroscopy" refers to spectroscopy of a working catalyst in combination with on-line activity measurements, while "in situ spectroscopy" refers to spectroscopy of a material under specific conditions, not necessarily reaction conditions [55].

The catalysts were continuously monitored by optical fiber UV–vis spectroscopy in the diffuse reflectance mode. A schematic representation of the setup is given in Fig. 1. The setup consists of a plug-flow reactor fitted inside a furnace, a UV–vis light source (Top Sensor Systems DH-2000 deuterium–halogen light source) and a photodiode

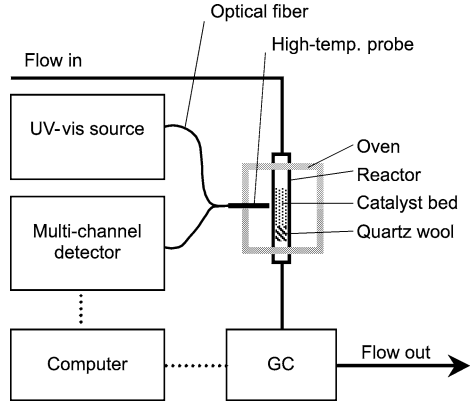

Fig. 1. Scheme of the fiber optic UV–vis spectrometer and reactor setup.

array detector (Ocean Optics SD 2000) connected to the catalyst bed via optical fiber technology (Top Sensor Systems FCB-UV400-ME cable and FCB-UV400G-0.1-XHT high-temperature probe). An optimal signal/noise ratio of the spectra was found when the high-temperature probe is placed in the reactor itself about 1 mm above the catalyst bed [57]. However, it turned out that the uppermost layer of the catalyst bed is not always representative for the bulk and an alternative position of the high-temperature probe was used. As shown in Fig. 1, the probe was mounted outside the reactor and spectra were collected through the quartz reactor wall. Before each new experiment, the UV–vis spectrum of a reactor containing hydrated Na-ZSM-5 was recorded and subsequently subtracted of all measured Cu-ZSM-5 spectra. Typically, one spectrum in the 38,000–12,000 cm^{-1} region is the result of the superposition of 5000 scans, each taking 50 ms. The signal/noise ratio of the spectra markedly deteriorated during the course of this study, which was due to the aging of the high-temperature probe. When the time period of the experiment amounted to days rather than minutes, major differences in the total intensities of the different spectra could be found. In these cases (Figs. 5b and 9b), the individual spectra were rescaled with respect to the most intense absorption band, i.e., ca. 33,000 cm^{-1}. The latter action is justified as (1) the intensity change of the 30,000 cm^{-1} band is definitely inferior to that of the 21,500 cm^{-1} band (see Fig. 3) and (2) the discussion of Figs. 5b and 9b only concerns the relative intensity of the 21,500 cm^{-1} band. Throughout the discussion, the intensity of the 21,500 cm^{-1} band is used as a measure of the amount of bis(μ-oxo)dicopper core. Since we do not yet have a method to quantify the amount of bis(μ-oxo)dicopper core, it was not possible to make a calibration line, relating the 21,500 cm^{-1} peak intensity to the bis(μ-oxo)dicopper concentration. Therefore, the discussion is based on relative rather than absolute bis(μ-oxo)dicopper concentrations. We are aware of the fact that also the temperature influences the bandwidth and intensity of the 21,500 cm^{-1} band (see Fig. 2). However, the latter temperature effect on the 21,500 cm^{-1} band intensity is inferior to those related to catalysis.

In situ DRS spectra of the series of Cu-ZSM-5 samples with increasing Cu content were recorded on a Varian Cary 5 UV–vis–NIR spectrophotometer. The samples (pellets of 0.25–0.4 mm) were brought into quartz flow cells, which have a suprasil window for DRS measurements. After overnight calcination (heating rate of 2 K min^{-1} to 723 K; O_2 flow of 50 ml min^{-1}), the samples were cooled in O_2 atmosphere, flushed with He (1 min at RT), and measured with DRS at RT. The spectrum of dehydrated Na-ZSM-5 was subtracted of all Cu-ZSM-5 spectra. We emphasize that in order to stabilize the bis(μ-oxo)dicopper core in the calcined sample, cooling should be done in a closed O_2 atmosphere and recording spectra should always be done in situ (in order to eliminate all possible traces of H_2O which immediately convert the core in a bis(μ-hydroxo)dicopper core).

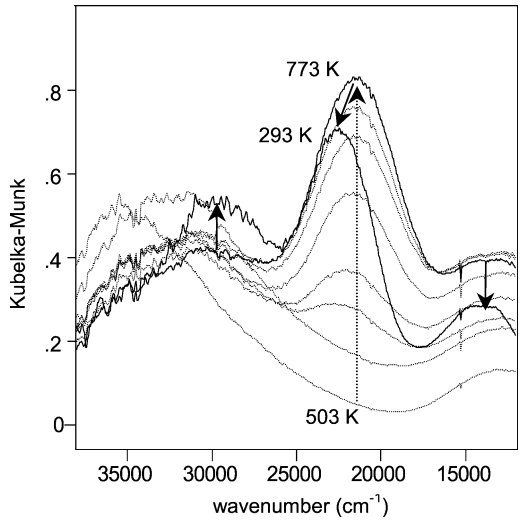

Fig. 2. Evolution of the in situ UV–vis spectra of CZ-31-0.58 during calcination. Dotted lines represent the spectra collected at 503, 603, 633, 673, 743, 773, and 773 K (15 min). Full lines represent the spectra collected after 2 h at 773 K and after cooling to room temperature in O_2 atmosphere.

3. Results

3.1. O_2-activated Cu-ZSM-5 and temperature dependence of the CT band positions

Fig. 2 shows the evolution of the in situ UV–vis spectra of CZ-31-0.58 collected during calcination. Below 623 K, a broad band centered at about 35,000 cm^{-1} and a weaker band at 13,000 cm^{-1} characterize the sample. These bands are ascribed to respectively $O_{zeolite} \rightarrow$ Cu(II) CT transitions and *d–d* transitions of (partially hydrated) Cu(II) ions, in agreement with literature UV–vis data [58] and our previous XAFS characterizations of the samples [49]. Above 623 K, a band at 21,500 cm^{-1} is found, the intensity of which increases with calcination time. A shift of the 35,000 cm^{-1} band to 30,000 cm^{-1} can also be distinguished. Upon cooling to room temperature, the 21,500 cm^{-1} band shifts to 22,500 cm^{-1}. The intense 22,500 cm^{-1} band and the weak 30,000 cm^{-1} band are identical to those detected in our previous UV–vis measurement (at RT) of calcined Cu-ZSM-5 [49] and are ascribed to the ELO $\rightarrow$ Cu CT transitions of the bis(μ-oxo)dicopper core [49].

Fig. 3 shows the spectral changes upon switch from a 100 mol% O_2 flow to a 1 mol% NO in He flow at 773 K. This set of spectra was collected with the probe in the reactor, just above the catalyst bed. It is clearly monitored that the intensities of the bands at 21,500 cm^{-1} and 30,000 cm^{-1} gradually decrease upon NO/He flushing, and that the 13,000 cm^{-1} band intensity increases. Thus, the 21,500 and 30,000 cm^{-1} bands of the calcined sample behave equally and can indeed be assigned to a single Cu-ELO species, identified previously as bis(μ-oxo)dicopper [49]. The interpretation of the 13,000 cm^{-1} band will be discussed further in the paper.

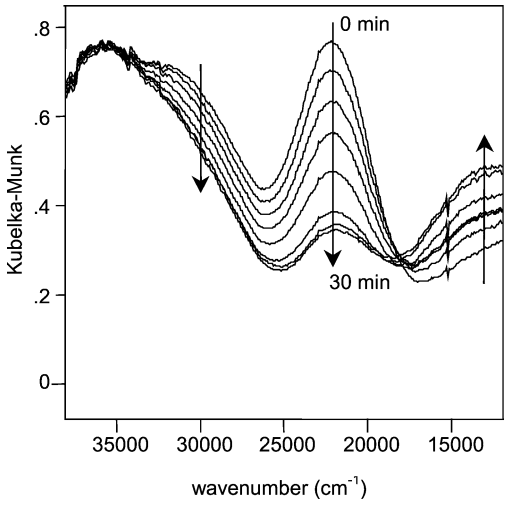

Fig. 3. In situ UV–vis spectra of CZ-31-0.58 at 773 K during switch from 100 mol% O_2 to 1 mol% NO/He flow. At 0 min the flows were switched and spectra were recorded every 4 min 15 s.

3.2. Time and temperature dependence of the NO decomposition

Figs. 4a and b give the evolution of the reactor outlet composition and the UV–vis spectra as a function of time, when 1 mol% NO in He is admitted to the pretreated catalyst at 773 K. The spectrum of CZ-31-0.58 pretreated in He at 773 K for 4 h is indicated with the label "0 min." The latter spectrum consists of a broad intense band with maximum absorbance at 33,400 cm^{-1}. Previous studies [58,59] have attributed the absorption bands at around 35,700–33,300, and 33,300–31,200 cm^{-1} to the electronic excitation of the Cu^+ ion ($3d^{10} \rightarrow 3d^9 4s^1$) and the Cu^+Cu^+ dimer ($3\sigma^* \rightarrow 3\sigma$) respectively. As a result, the observed 33,400 cm^{-1} band can be explained by the presence of Cu^+ monomers, Cu^+Cu^+ dimers, or a mixture of them. Alternatively, an absorption band at ca. 30,000 cm^{-1} could also be due to the presence of divalent copper species such as $[CuOCu]^{2+}$, $Cu^{2+}O^-$ and $Cu^{2+}O_2{}^-$ [40,58,60,61]. But, no clear bands at lower energy (*d–d* bands) are distinguished, making the presence of divalent copper species unlikely. The latter is confirmed by the corresponding XANES spectrum of this pretreated sample, showing Cu(I) and no Cu(II) near-edge peaks [49]. These findings together with the corresponding EXAFS data [49], showing a Cu···Cu contribution at 2.84 Å with coordination number of 0.5, indicates the presence of a mixture of Cu^+ monomers and Cu^+ Cu^+ dimers after He pretreatment. This conclusion is shared by previous XAFS studies on pretreated Cu-ZSM-5 samples [62,63]. The presence of a major amount of Cu_2O nanoparticles is not plausible since (1) their characteristic bandgap transition (at energy $\geqslant$ 16,200 cm^{-1}) cannot be discerned in our UV–vis spectra and (2) an EXAFS Cu···Cu separation of 2.84 Å is observed rather than the characteristic Cu···Cu separation of 3.01 Å of Cu_2O.

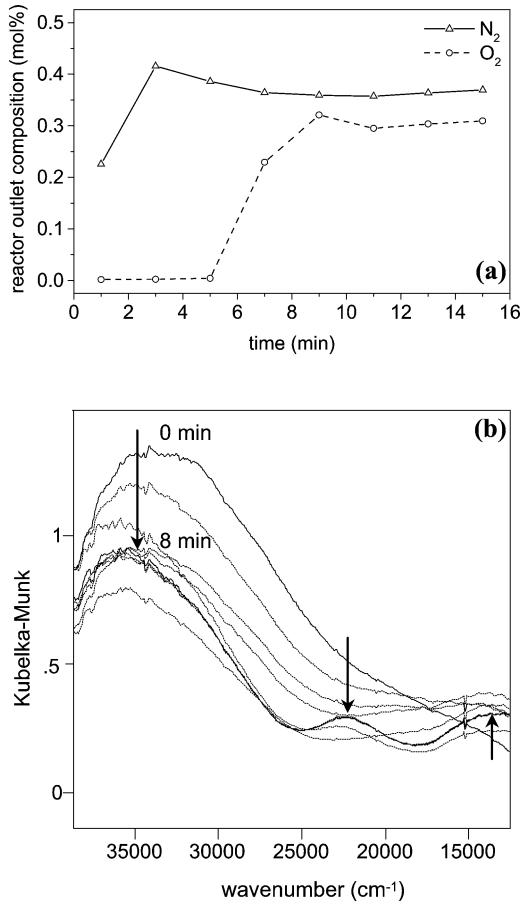

Fig. 4. (a) Evolution of the reactor outlet composition of CZ-31-0.58 upon admission of 1 mol% NO in He at 773 K (900 h^{-1} GHSV). (b) Corresponding evolution of the operando UV–vis spectra. "0 min" corresponds with the pretreated sample in He and spectra were recorded every 1 min and 1000 scans of 50 ms constitute one spectrum.

Fig. 4a shows that upon exposure of NO, immediately a high N_2 yield is obtained, while the O_2 yield is almost zero. After about 7 min, also a high O_2 yield is found and after 15 min, the N_2 and O_2 yields amount to 74 and 62%, respectively (i.e., in a 5% margin of their steady-state values). Fig. 4b shows that in the presence of NO the intensity of the 33,400 cm^{-1} band decreases and that after 3 and 6 min a band appears at 13,000 cm^{-1} and 21,500 cm^{-1}, respectively. As a result, the interaction of NO with the Cu(I) sample causes a partial conversion of Cu(I) to (1) the bis(μ-oxo)dicopper core and (2) a second copper species, which identification will be discussed further. It is clear that the formation of the bis(μ-oxo)dicopper core after about 6 min is concomitant to the steady-state approach of the reaction.

The steady-state catalytic activity of CZ-31-0.58 as a function of the temperature and the corresponding UV–vis spectra are shown in Figs. 5a and 5b, respectively. The highest N_2 yield, amounting to 77%, was obtained at 773 K and a gradual loss in activity is observed upon decreasing the reaction temperature. In the 773–623 K range, the O_2 yield is

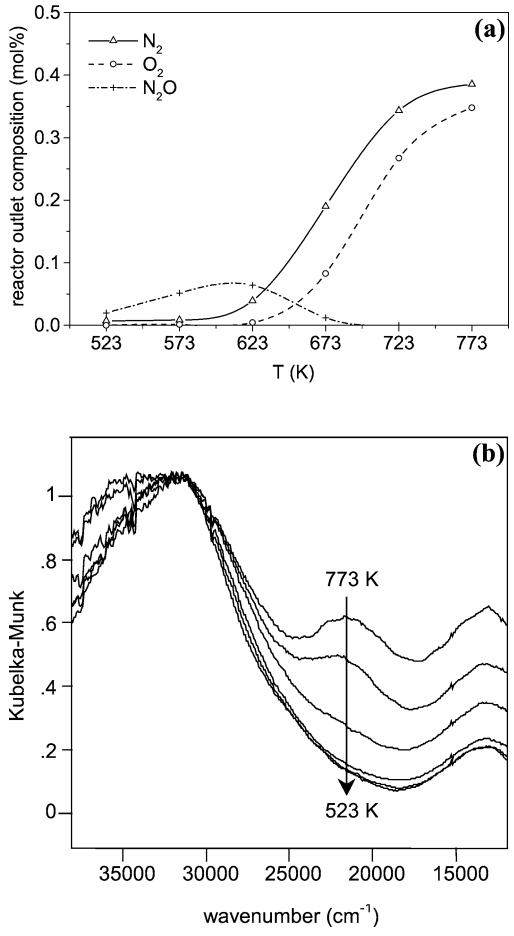

Fig. 5. (a) Catalytic activity of CZ-31-0.58 for the decomposition of NO (1 mol% in He; 900 h^{-1} GHSV) as function of the temperature. (b) Corresponding operando UV–vis spectra at temperature intervals of 50 K.

always lower than the N_2 yield, by a value of about 10%. In correspondence with the literature [21,24], the latter discrepancy can be assigned to the reaction of produced O_2 with unreacted NO forming NO_2 in the cool exit zone of the reactor and in the GC. Below 673 K, the formation of N_2O is observed with a maximum yield at 623 K. At 773 K, the TOF (molecules NO converted to N_2 per hour per Cu atom) amounts to 1.8 h^{-1}. Additional catalytic results of this CZ-31-0.58 sample and of a sample with $Si/Al = 12$ can be found in a recent contribution of our group [49] where also the effluent NO and NO_2 concentrations were monitored using a NO_x analyzer. In the latter study, a 100% selective NO decomposition to O_2 and N_2 was obtained for a 0.1 mol% NO in He flow (GHSV of 900 h^{-1}) in the temperature range from 773 to 723 K. The catalytic results of our Cu-ZSM-5 samples are in agreement with the literature data [21,23,40]. New information is obtained with the concomitant UV–vis monitoring. Fig. 5b shows that the band at 21,500 cm^{-1} is quite intense at 773 and 723 K, very weak at 673 K, and absent at lower temperature. Thus, the amount of bis(μ-oxo)dicopper decreases with decreasing reaction temperature in qualitative agreement with the catalytic activity drop.

3.3. NO decomposition activity as a function of the copper content of Cu-ZSM-5

Fig. 6a shows the reactor outlet composition for the CZ-12 series of samples when contacted with a 1 mol% NO in He inlet flow at 15 ml min^{-1} (GHSV of 900 h^{-1}). In Fig. 6b, the analogue is shown for a 2 mol% NO in He inlet flow at 45 ml min^{-1} (GHSV of 2700 h^{-1}). The data points are also summarized in Table 2, together with two additional experiments (2 mol% NO and GHSV of 900 h^{-1}; 1 mol% NO and GHSV of 2700 h^{-1}). Both Figs. 6a and 6b show that the N_2 and O_2 yields (1) are low for the samples with Cu/Al ratios of 0.10 and 0.22, (2) sharply increase for the Cu/Al 0.31 sample, and (3) further increase for the higher Cu/Al ratios. In 1991, Iwamoto et al. [23] were the first to report this sharp increase in activity for samples with $Cu/Al > 0.2$. In order to estimate the amount of bis(μ-oxo)dicopper in the CZ-12 series of samples, the UV–vis–NIR spectra were collected after calcination and are shown in Fig. 7. For the samples with Cu/Al ratio's of 0.10 and 0.22, no band at 22,700 cm^{-1} can be discerned (within the accuracy of the technique), while it appears in the spectrum of the $Cu/Al = 0.31$ sample and grows for the higher copper loadings. In fact, the intensity of the 22,700 cm^{-1} band, and thus the amount of bis(μ-oxo)dicopper, nicely corresponds with the catalytic NO decomposition activity. As noted before [49], the intensity of the 6200 cm^{-1} band increases equally with that of the 22,700 cm^{-1} band, suggesting that they originate from the same copper species. Figs. 6c and 6d give the corresponding TOF (molecules NO converted to N_2/O_2 per hour per Cu atom) as function of the Cu/Al ratio. The latter profiles similarly show the sharp increase between Cu/Al 0.2 and 0.3. Finally, let us compare the TOF of the most active sample without bis(μ-oxo)dicopper (i.e., $Cu/Al = 0.22$) with that of the most active sample containing the bis(μ-oxo)dicopper core (i.e., $Cu/Al = 0.58$). Then, Fig. 6d shows that the average Cu atom in the sample with Cu/Al 0.58 is respectively 4.3 and 20.1 times more active for conversion of NO to N_2 and O_2 when compared to the sample with Cu/Al 0.22. These findings additionally prove the key role of the bis(μ-oxo)dicopper core in the catalytic NO decomposition over Cu-ZSM-5.

3.4. NO decomposition activity as a function of the O_2 content in the feed

The effect of O_2 in the reactant stream on the NO decomposition activity and on the operando UV–vis spectra of CZ-31-0.58 at 773 K is illustrated in Figs. 8a and 8b, respectively. Fig. 8a shows a continuous decrease of the N_2 yield as the amount of O_2 in the feed increases. No N_2O was detected. When O_2 addition is stopped, the initial activity was regained as indicated with the asterisk in Fig. 8a.

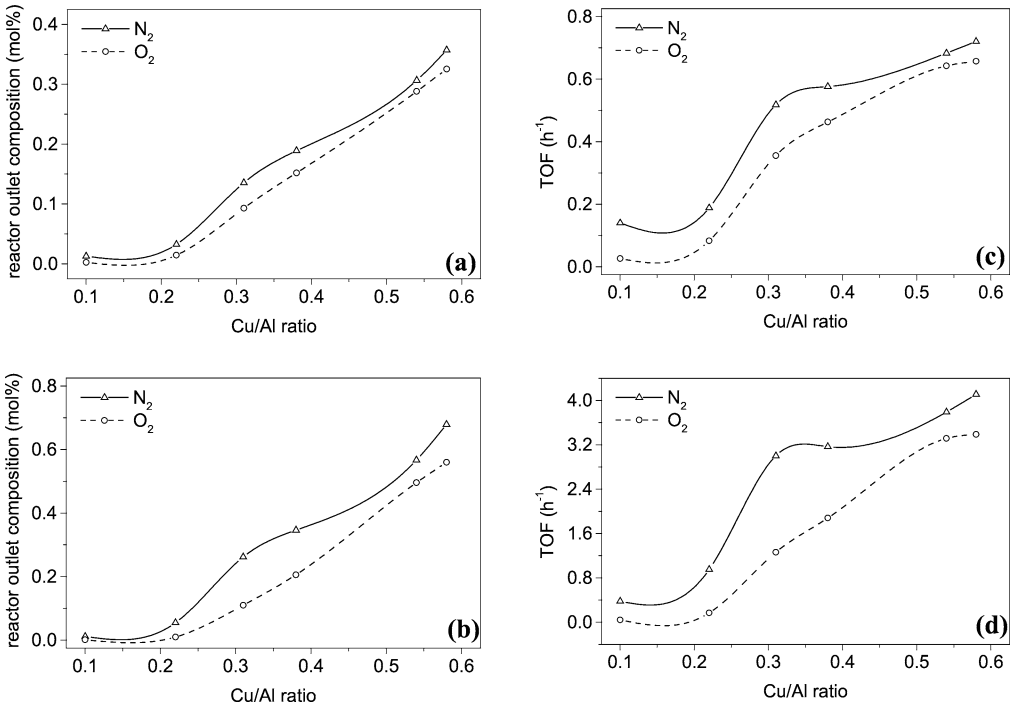

Fig. 6. Catalytic activity as function of the Cu/Al ratio of the CZ-12 series of samples: (a) contacted with 1 mol% NO in He (900 h^{-1} GHSV); (b) contacted with 2 mol% NO in He (2700 h^{-1} GHSV). TOF (toward N_2 and O_2) as function of the Cu/Al ratio of the CZ-12 series of samples: (c) contacted with 1 mol% NO in He (900 h^{-1} GHSV); (d) contacted with 2 mol% NO in He (2700 h^{-1} GHSV).

Table 2
Catalytic results of CZ-12 series of samples

Cu/Al	Inlet: 1 mol% NO; 900 h^{-1}		Inlet: 2 mol% NO; 900 h^{-1}		Inlet: 1 mol% NO; 2700 h^{-1}		Inlet: 2 mol% NO; 2700 h^{-1}	
	Outlet N_2 (mol%)	Outlet O_2 (mol%)	Outlet N_2 (mol%)	Outlet O_2 (mol%)	Outlet N_2 (mol%)	Outlet O_2 (mol%)	Outlet N_2 (mol%)	Outlet O_2 (mol%)
0.10	0.0128	0.0024	0.0247	0.0022	0.0048	0.0013	0.0115	0.0013
0.22	0.0326	0.0144	0.0895	0.0198	0.0196	0.0084	0.0549	0.0097
0.31	0.1355	0.0930	0.3305	0.1711	0.1023	0.0645	0.2617	0.1100
0.38	0.1891	0.1520	0.4261	0.3022	0.1436	0.1067	0.3464	0.2057
0.54	0.3066	0.2882	0.6205	0.5660	0.2567	0.2336	0.5670	0.4959
0.58	0.3572	0.3256	0.7373	0.6367	0.3119	0.2719	0.6793	0.5600

The corresponding UV–vis spectra show that with increasing O_2 concentration, the intensity of the 21,500 cm^{-1} band increases while the 13,000 cm^{-1} band intensity decreases. This results in an isosbestic point at 19,000 cm^{-1}. Further, at ca. 30,000 cm^{-1} an intensity raise, which is proportional to the 21,500 cm^{-1} band increase, can be discerned with increasing O_2 concentration. Fig. 8b also shows that after setting the O_2 concentration in the feed back to 0 mol%, the obtained spectrum coincides with the initial spectrum obtained at 0 mol% O_2. A closer inspection of Figs. 8a and 8b shows that the reactivity decrease and intensity increase of the 21,500 cm^{-1} band are most pronounced for the initial increase in O_2 concentration from 0 to 2 mol% O_2. Consequently, in this experiment the concentration of the bis(μ-oxo)dicopper core displays an inversely proportional relation to the NO decomposition activity of the sample.

3.5. Temperature dependence of the N_2O decomposition

In Fig. 9a the activity of the CZ-31-0.58 sample for the decomposition of N_2O (1 mol%) is depicted as a function of the temperature. In the temperature range from 773 to 673 K, N_2O is fully converted to N_2 and O_2. Below 673 K the conversion sharply drops and is almost zero at 523 K. Over the whole temperature range the molar ratio N_2:O_2 is 2:1. The corresponding operando spectra are shown in Fig. 9b. The spectra collected at 773, 723, and 673 K are roughly equal and exhibit a clear band at 21,500 cm^{-1}. The latter band is seriously reduced at 623 K and absent at 523 K. Therefore, the intensity of the 21,500 cm^{-1} band, i.e., the amount of the bis(μ-oxo)dicopper core, shows a very close correlation with the N_2O decomposition activity.

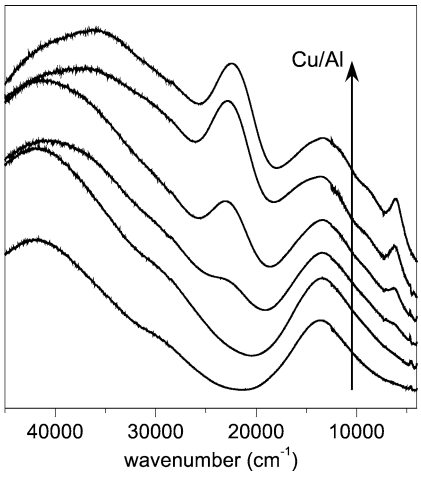

Fig. 7. Vertical stacking of the in situ UV–vis–NIR spectra of the calcined CZ-12 series of samples with increasing Cu/Al ratio: Cu/Al = 0.10, Cu/Al = 0.22, Cu/Al = 0.31, Cu/Al = 0.38, Cu/Al = 0.54, and Cu/Al = 0.58.

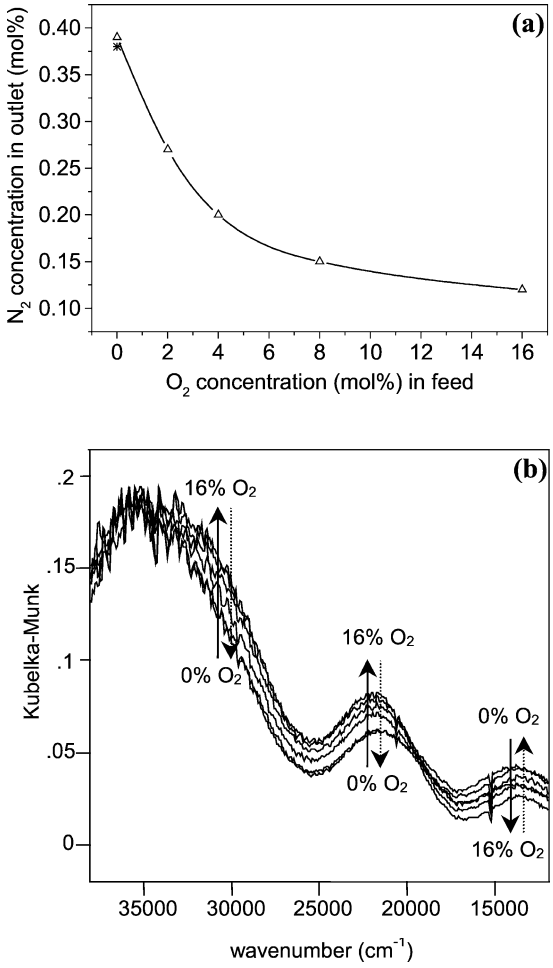

Fig. 8. (a) Catalytic activity of CZ-31-0.58 for the decomposition of NO (1 mol%; 900 h^{-1} GHSV) at 773 K as function of the O_2 concentration in the feed. After feeding 16 mol% O_2, the O_2 concentration was again set to 0 mol% and the asterisk gives the corresponding activity. (b) Corresponding operando UV–vis spectra.

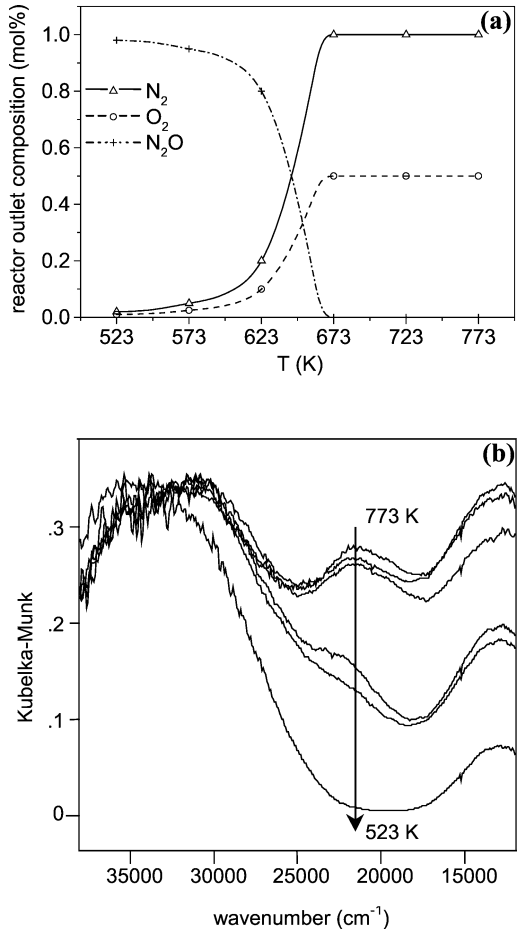

Fig. 9. (a) Catalytic activity of CZ-31-0.58 for the decomposition of N_2O (1 mol%; 900 h^{-1} GHSV) as function of the temperature. (b) Corresponding operando UV–vis spectra at temperature intervals of 50 K.

3.6. N_2O decomposition activity as a function of the O_2 content in the feed

In analogy to the study of the NO decomposition activity, the N_2O decomposition activity and concomitant UV–vis spectra were monitored while increasing the O_2 concentration in the inlet from 0% to 16 mol%. In contrast to the NO decomposition behavior, no decrease of the N_2O conversion was found, which remained constantly 100% while feeding 1, 2, or 3 mol% N_2O and 0–16 mol% O_2 at 773 K. The concomitant UV–vis spectra reveal an increase of the 21,500 cm^{-1} band with increasing O_2 concentration and are similar to the spectra of Fig. 8, obtained in the analogous NO decomposition experiment.

3.7. N_2O decomposition during temperature drop

Figs. 10a and 10b illustrate the effect of a temperature drop respectively on the N_2O decomposition activity and the operando UV–vis spectra of CZ-31-0.58. At Time 0 the temperature was decreased from 723 to 673 K at a rate of 5 K min^{-1} so that after 10 min the final temperature of 673 K was reached. During the whole experiment the N_2

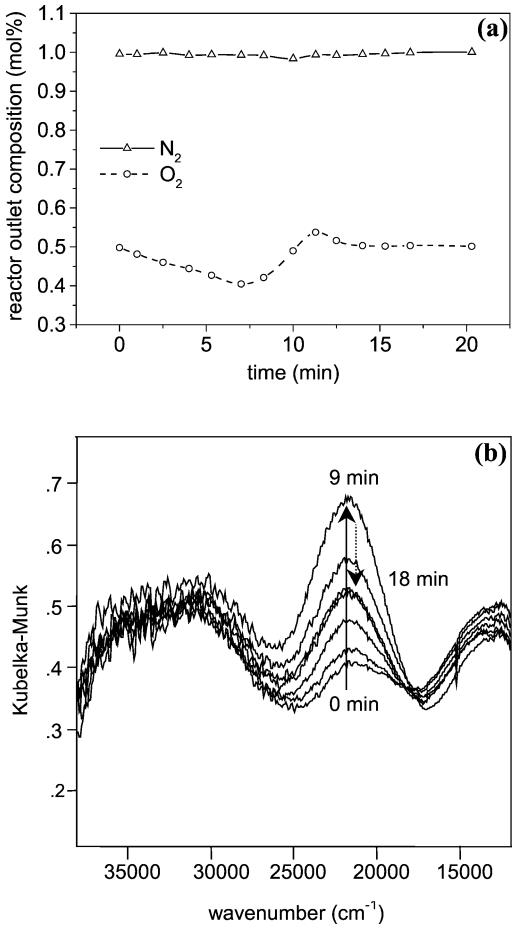

Fig. 10. (a) Catalytic activity of CZ-31-0.58 for the decomposition of N_2O (1 mol%; 900 h^{-1} GHSV) during the temperature switch from 723 to 673 K. At 0 min the temperature decrease of 5 K min^{-1} was started. (b) Corresponding operando UV–vis spectra (spectra were recorded every 3 min and 1000 scans of 50 ms constitute one spectrum).

concentration detected in the outlet is constant and close to 1 mol%, consistent with a full conversion of 1 mol% N_2O in the inlet. The O_2 concentration in the effluent is below the steady-state value of 0.5 mol% during the first 10 min, indicating retention of oxygen. In the concomitant UV–vis spectra a sharp rise of the 21,500 cm^{-1} band is observed, with maximum intensity after 9 min. As a result, the combination of the GC and operando UV–vis results indicates that around 10 min a maximum is reached in the accumulation of oxygen under the form of the bis(μ-oxo)dicopper core. At the end of the experiment, the 21,500 cm^{-1} band is still higher than in the initial spectrum collected at 723 K (0 min). Also this observation can nicely be explained by the GC results. Fig. 10a shows that the average O_2 concentration of the effluent is lower than 0.5 mol% during the course of the experiment. Thus, the catalyst contains more oxygen at minute "20" compared to minute "0," which is also reflected in the 21,500 cm^{-1} band intensity, i.e., the concentration of the bis(μ-oxo)dicopper core.

Is the above discussed retention of oxygen during N_2O decomposition and cooling due to (1) the adsorption of gas-phase O_2 onto the catalyst or (2) the slowing down of the O_2 release step in the N_2O decomposition cycle? To answer this question, the CZ-31-0.58 sample was cooled down from 723 to 673 K at 5 K min^{-1}, in an atmosphere of 2 mol% O_2 in He. In this case, no such an increase of the 21,500 cm^{-1} band intensity was observed. Thus, the answer is that the accumulation of the bis(μ-oxo)dicopper core during the N_2O decomposition and temperature switch is not due to an enhanced incorporation of gaseous O_2. Rather, the oxygen atoms abstracted from N_2O are incorporated in the bis(μ-oxo)dicopper core, and the subsequent retarded release of produced O_2 from this core causes its accumulation.

4. Discussion

4.1. Bis(μ-oxo)dicopper formed by O abstraction of N_2O

In the discussion of the catalytic performance of Cu-ZSM-5 for the NO decomposition, two temperature intervals can be defined. At 673–773 K, a 38–77% N_2 yield is found for a 1 mol% NO feed, while no N_2O yield is detected. Below 673 K, the N_2O yield rapidly increases and exceeds the N_2 yield at $\leqslant$ 623 K. This finding is in accordance with previous studies, which inferred that N_2O is an intermediate in the NO decomposition cycle [23,40,43,45]. Studying the N_2O decomposition activity as function of the temperature (Fig. 9a), showed that the conversion of 1 mol% N_2O to N_2 and O_2 is complete at 673–773 K but amounts only to 20% at 623 K. Thus, in both the NO and the N_2O decomposition cycle, the conversion of N_2O is strongly retarded below 673 K.

Also in the operando UV–vis spectra of Cu-ZSM-5 during decomposition of NO and N_2O, a clear temperature dependency is observed. Figs. 5 and 9 show that the intensity of the 21,500 cm^{-1} band, i.e., the bis(μ-oxo)dicopper concentration, is highest in the 673–773 K range and thus proportional to the N_2 yield. In case of the N_2O decomposition, the sharp and concomitant decrease of (1) N_2O conversion and (2) the amount of bis(μ-oxo)dicopper is very clearly observed upon lowering the temperature below 673 K. This finding suggests that bis(μ-oxo)dicopper is formed by O abstraction of N_2O and that this reaction is strongly retarded below 673 K. However, some caution is necessary, since the calcination experiments (Figs. 2 and 3) showed that bis(μ-oxo)dicopper is also formed in O_2 atmosphere. As a result, the close correlation between bis(μ-oxo)dicopper concentration and decomposition activity could also result from bis(μ-oxo)dicopper core formation by incorporation of gaseous O_2 (the latter produced by another Cu site), rather than by the direct route of O abstraction of N_2O. In order to examine whether bis(μ-oxo)dicopper is an active site or a spectator species, experiments under transient reaction conditions were performed. Fig. 10 showed that a sudden temperature drop during N_2O decomposition had no effect on the N_2 yield, which remained consistent with full N_2O conversion,

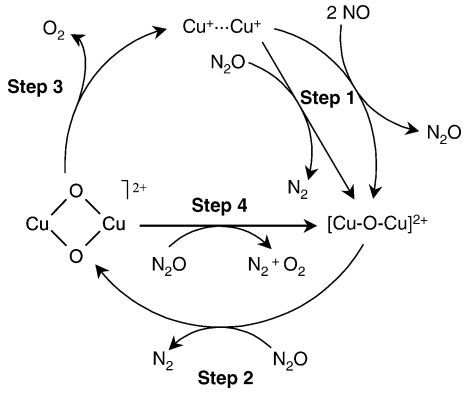

Scheme 1. Proposed reaction mechanism for the decomposition of NO and N_2O.

but did cause a retention of O_2 under the form of bis(μ-oxo)dicopper. By performing a parallel experiment, where O_2 rather than N_2O was fed, it was shown that the latter accumulation of the bis(μ-oxo)dicopper core is not caused by an enhanced incorporation of gaseous O_2. Thus, during N_2O decomposition, the bis(μ-oxo)dicopper core is mainly formed by the abstraction of oxygen atoms from N_2O, and the subsequent retarded release of O_2 from this core causes its accumulation during temperature switch. In summary, very strong indication is found that the bis(μ-oxo)dicopper core is an active site during the NO and N_2O decomposition reactions. Scheme 1 shows our proposed NO/N_2O decomposition cycle that is consistent with the copper intermediates detected by operando UV–vis and XAFS [49]. The scheme shows that bis(μ-oxo)dicopper and N_2 are formed by O abstraction of N_2O (step 2) and that bis(μ-oxo)dicopper subsequently fulfills the role of O_2 release (step 3).

4.2. O_2 release from bis(μ-oxo)dicopper

The finding that the TOF (of NO toward O_2) is 20 times higher for the CZ-12-0.58 sample (with bis(μ-oxo)dicopper) than for the CZ-12-0.22 sample (without bis(μ-oxo)dicopper) supports the assignment of the enhanced O_2 release capacity of Cu-ZSM-5 to the presense of the bis(μ-oxo)dicopper core. The O_2 release from bis(μ-oxo)dicopper, i.e., step 3 in Scheme 1, was further examined by adding O_2 to the reactant stream during NO decomposition (Fig. 8) and N_2O decomposition. For the NO decomposition, the activity was clearly retarded upon increasing the O_2 concentration. Concomitantly, an increase of the 21,500 cm^{-1} band, i.e., the amount of bis(μ-oxo)dicopper core, was observed and this effect was proportional to the activity decrease. These observations support the following two conclusions. First, the close correlation between the intensity of the bis(μ-oxo)dicopper spectrum and the NO decomposition activity again strongly indicates that this Cu species is an intermediate in the reaction cycle. Second, the increasing bis(μ-oxo)dicopper concentration with increasing surrounding O_2 concentration (and concomitant decreasing activity) suggests that step 3 can be reversed at this temperature. This reversible conversion between $Cu^+\cdots Cu^+$ and bis(μ-oxo)dicopper was also observed when flowing consecutively O_2 and He at 773 K. Thus in the above experiment, an increased surrounding O_2 concentration results in a higher fraction of bis(μ-oxo)dicopper units and a smaller amount of available $Cu^+\cdots Cu^+$ pairs, leading to a decreased NO decomposition activity. As was discussed in the Introduction, it is known that the Cu(I) concentration correlates with the NO decomposition rate [32]. Finally, the fact that the retardation of the O_2 release step causes a retardation of the reaction cycle strongly indicates that O_2 release of the bis(μ-oxo)dicopper core with regeneration of the $Cu^+\cdots Cu^+$ pair (step 3) is rate limiting in the NO decomposition. This conclusion can be shared by our recent XANES and EXAFS results pointing to the presence of a considerable fraction of the bis(μ-oxo)dicopper core during NO decomposition [49]. The O_2 inhibition effect on the NO decomposition over Cu-ZSM-5 is well known and has been incorporated in the rate equation containing an $[O_2]^{1/2}$ term in the denominator [34, 43]. In contrast, during N_2O decomposition in the presence of an increased O_2 concentration, also an increase of bis(μ-oxo)dicopper core concentration was observed but no decrease of reaction rate was found. A possible explanation for this different behavior will be discussed further in the paper.

4.3. The reaction cycle for NO decomposition

Feeding NO to Cu-ZSM-5 below 673 K results in a small N_2 yield and a considerable N_2O yield, suggesting that step 2 is unfavorable at this temperature. Thus, an accumulation of the intermediate Cu species, at the start of step 2, is expected. The corresponding operando spectra collected below 673 K (Fig. 5b) exhibit *d–d* transitions around 13,000 cm^{-1} and charge-transfer bands above 30,000 cm^{-1}. The $[CuOCu]^{2+}$ core is a good candidate for explaining the latter spectrum as this single-O-bridged Cu pair in synthetic model complexes is characterized by *d–d* transitions around 14,000 cm^{-1} and charge-transfer bands above 30,000 cm^{-1} [64]. As shown in Scheme 1, it is proposed that a $Cu^+\cdots Cu^+$ pair reacts with 2 NO molecules producing $[CuOCu]^{2+}$ and N_2O. In Fig. 4b, showing the UV–vis spectra collected during the admission of NO to the pretreated sample, the formation of the 13,000 cm^{-1} band precedes that of the 21,500 cm^{-1} band. This observation is consistent with the proposed cycle for NO decomposition (Scheme 1) in which the $[CuOCu]^{2+}$ core formation precedes the $[Cu_2(\mu\text{-}O)_2]^{2+}$ core formation. An isosbestic point between the 13,000 and 21,500 cm^{-1} bands was observed in Fig. 3. Concomitant to the decrease of the 21,500 cm^{-1} band of $[Cu_2(\mu\text{-}O)_2]^{2+}$, as a result of the drop of the O_2 concentration, an intensity increase of the 13,000 cm^{-1} band of $[CuOCu]^{2+}$ is observed, the latter formed by the conversion of NO. The presence of the isosbestic point in Fig. 8 indicates that the surrounding O_2 concentration is an important factor in the equilibrium concentrations of the $[CuOCu]^{2+}$ and $[Cu_2(\mu\text{-}O)_2]^{2+}$ cores.

All three copper intermediates of Scheme 1 were identified with operando UV–vis spectroscopy by blocking one of the steps, e.g., by playing on the temperature or equilibrium conditions, causing the accumulation of one of the three intermediates. After pretreatment at elevated temperature in He the obtained spectrum is consistent with the presence of $Cu^+\cdots Cu^+$ pairs. Upon admission of NO below 673 K, the formation of N_2O and $[CuOCu]^{2+}$ is observed; i.e., step 1 occurs and step 2 is retarded. Above 673 K, a high steady-state decomposition of NO into N_2 and O_2 is observed together with the $[Cu_2(\mu\text{-}O)_2]^{2+}$ formation. Step 3 could be reversed or retarded by respectively increasing the surrounding O_2 concentration or suddenly dropping the temperature, causing an accumulation of the bis(μ-oxo)dicopper core. Thus, the observations firmly suggest that (1) below 673 K, step 2 (N_2O decomposition) is rate limiting and (2) above 673 K, step 3 (O_2 desorption) is rate limiting. This, in turn, strongly suggests that the activation energy for N_2O decomposition is higher than that of O_2 desorption.

The proposed catalytic cycle is also theoretically supported. The reaction energies of each of the individual reaction steps shown in Scheme 1 were calculated in DFT (density functional theory) studies of Goodman et al. [38] and Sengupta et al. [65]. In the latter DFT studies, the zeolite environment was represented by $[Al(OH)_4]^-$ tetrahedrons, to which Cu is twofold coordinated. It must be noted that the type of geometric isomer of the Cu_2O_2 core was not specified and it can thus be one of the three low-energy geometric isomers: bis(μ-oxo)dicopper, planar (μ-η^2:η^2-peroxo)dicopper, and *trans*(μ-1,2-peroxo)dicopper. All reaction steps shown in Scheme 1 were found to be exothermal, with the exception of the release of O_2 [38,65].

The routes for N_2O and N_2 formation, as included in step 1 of Scheme 1, are in good agreement with NO decomposition pathways postulated on the basis of infrared and transient reduction and reaction studies [21,33,43]. Nevertheless, we want to stress that the presented UV–vis technique does not offer supporting information for the reaction mechanism of step 1, i.e., the chemisorption of NO and the N-pairing reaction. It is not proven by the presented results that $Cu^+\cdots Cu^+$ pairs are necessary for the formation of N_2O, i.e., the formation of N_2O might also occur on only one of the Cu^+ ions of the pair. Coming to O_2 formation, several pathways are postulated in literature, probably due to the lack of spectroscopic information on the adsorbed oxygen species [45]. Based on the DFT study of Goodman et al. [38], $[CuO_2Cu]^{2+}$ species were incorporated in recent NO decomposition schemes proposed by Iglesia and co-workers [43] and Chuang and co-workers [66]. In the study of Iglesia and co-workers [43] it was suggested that the conversion of two $[CuOCu]^{2+}$ cores into one $[CuO_2Cu]^{2+}$ core is mediated by NO and NO_2. In the present contribution we present the first spectroscopic identification of a $[CuO_2Cu]^{2+}$ core on Cu-ZSM-5, that is, the $[Cu_2(\mu\text{-}O)_2]^{2+}$ core, and have strong evidence for its formation by O abstraction of N_2O.

The identification of bis(μ-oxo)dicopper as intermediate might also offer an explanation for the suppression of the NO decomposition activity of Cu-ZSM-5 in the presence of water vapor. Iwamoto et al. [23] found that the NO decomposition activity was reduced in the presence of H_2O but again regenerated by its absence. This reversible effect was also observed in our laboratory and simultaneously with the reduced activity, a decrease of the 21,500 cm^{-1} band was found. It is known that the bis(μ-oxo)dicopper core exhibits high tendencies to abstract hydrogen atoms from substrates resulting in the formation of a bis(μ-hydroxy)dicopper core [50]. Instead of the CT band at 21,500 cm^{-1}, the latter core exhibits a $OH^- \rightarrow$ Cu(II) CT band at about 30,000 cm^{-1} [67]. In the context of NO decomposition, the formation of this bis(μ-hydroxy)dicopper might prohibit the reconstitution of the Cu^+–Cu^+ pairs, resulting in a retardation of the cycle.

4.4. The reaction cycle for N_2O decomposition

As discussed above, the reaction of N_2O with two Cu^+ ions forming N_2 and $[CuOCu]^{2+}$ was calculated to be highly exothermal in the DFT study of Goodman et al. [38]. Based on this fact and the present results, we included the latter reaction (step 1) in Scheme 1 yielding a closed catalytic cycle for the N_2O decomposition over Cu-ZSM-5.

The catalytic decomposition of N_2O over Cu-ZSM-5 differs from that of NO in at least two important points: (1) a considerably higher rate of N_2O decomposition compared to NO decomposition and (2) the lack of an O_2 inhibition effect on N_2O decomposition, in contrast to NO decomposition. Both facts were also observed in a recent study of Konduru and Chuang [45]. While we found the O_2 release step (step 3) to be rate limiting in the NO decomposition, the above characteristics of the N_2O decomposition reaction raise the idea that the latter reaction somehow bypasses step 3 and does not necessarily proceed via the $Cu^+\cdots Cu^+$ pairs. As a result, the presence of step 4 in Scheme 1, i.e., the reaction of $[Cu_2(\mu\text{-}O)_2]^{2+}$ with N_2O forming $[CuOCu]^{2+}$ and N_2 and O_2, could be a possible explanation for the present observations. Also step 4 was calculated in the DFT study of Sengupta et al. [65] and found highly exothermal.

5. Conclusions

Operando UV–vis spectroscopy combined with on-line GC analysis during the catalytic decomposition of NO by Cu-ZSM-5 leads to the identification of the bis(μ-oxo)dicopper core, $[Cu_2(\mu\text{-}O)_2]^{2+}$, as a key intermediate. Monitoring the catalytic conversion of NO and N_2O above 673 K strongly indicates that the bis(μ-oxo)dicopper core is formed by the O abstraction of the intermediate N_2O. Subsequently, bis(μ-oxo)dicopper fulfills the roles of O_2 production and release, guaranteeing the self-reduction of

the catalytic site. Studying the NO decomposition as a function of the O_2 content in the feed strongly suggests that O_2 release from bis(μ-oxo)dicopper is rate limiting in the NO decomposition at 773 K. Based on the present operando UV–vis data, our recent operando XAFS results [49] and the literature data, a reaction cycle for the NO decomposition is proposed, involving the intermediates: $Cu^+\cdots Cu^+$, $[CuOCu]^{2+}$, and $[Cu_2(\mu\text{-}O)_2]^{2+}$.

The O_2 release function can be seen as a key role in the NO decomposition cycle as most other materials tested for the NO decomposition are limited by the removal of the strongly adsorbed product oxygen. The suitability of the bis(μ-oxo)dicopper core for the O_2 release function can be explained by the fact that its peroxo-isomer, (μ-η^2:η^2-peroxo)dicopper, reversibly binds O_2 in the protein hemocyanin. So far, the presence of double-O-bridged Cu pairs in Cu-ZSM-5 was only postulated on the basis of the theoretical study of Goodman et al. [38]. With the present operando UV–vis and the recent operando XAFS contributions [49], we present the first experimental evidence for the formation of the bis(μ-oxo)dicopper core in Cu-ZSM-5 and for its key role in the sustained high activity of Cu-ZSM-5 in the direct decomposition of NO into N_2 and O_2.

Acknowledgments

T.A. Nijhuis of the Debye Institute, Utrecht University, is kindly acknowledged for the discussion of the kinetic data. This investigation has been supported by grants from the Fund for Scientific Research—Flanders (FWO-Vlaanderen) and from the Concerted Research Action of the Flemish Government (GOA). M.H.G. thanks the FWO-Vlaanderen for a postdoctoral fellowship.

References

[1] M. Shelef, Chem. Rev. 95 (1995) 209.
[2] K. Klier, R.G. Herman, S.L. Hou, Zeolites Relat. Micropor. Mater. 84 (1994) 1507.
[3] CRC Handbook of Chemistry and Physics, 3rd electronic ed., 2000.
[4] R.J. Wu, C.T. Yeh, Int. J. Chem. Kinet. 28 (1996) 89.
[5] M. Iwamoto, H. Furukawa, Y. Mine, F. Uemura, S.I. Mikuriya, S. Kagawa, J. Chem. Soc. Chem. Commun. (1986) 1272.
[6] J. Dedecek, O. Bortnovsky, A. Vondrová, B. Wichterlová, J. Catal. 200 (2001) 160.
[7] J. Dedecek, J. Cejka, B. Wichterlová, Appl. Catal. B 15 (1998) 233.
[8] Z. Schay, L. Guczi, Z. Koppany, I. Nagy, A. Beck, V. Samuel, M.K. Dongare, D.P. Sabde, S.G. Hegde, A.V. Ramaswamy, Catal. Today 54 (1999) 569.
[9] V.I. Pârvulescu, P. Grange, B. Delmon, Appl. Catal. B 33 (2001) 223.
[10] I. Sobczak, P. Decyk, M. Ziolek, M. Daturi, J.C. Lavalley, L. Kevan, A.A. Prakash, J. Catal. 207 (2002) 101.
[11] P.W. Park, J.K. Kil, H.H. Kung, M.C. Kung, Catal. Today 42 (1998) 51.
[12] Y. Teraoka, H. Fukuda, S. Kagawa, Chem. Lett. (1990) 1.
[13] F. Marquez, A.E. Palomares, F. Rey, A. Corma, J. Mater. Chem. 11 (2001) 1675.
[14] S.B. Xie, G. Mestl, M.P. Rosynek, J.H. Lunsford, J. Am. Chem. Soc. 119 (1997) 10186.
[15] G. Centi, S. Perathoner, Appl. Catal. A 132 (1995) 179.
[16] A. Dandekar, M.A. Vannice, Appl. Catal. B 22 (1999) 179.
[17] F. Kapteijn, G. Marbán, J. Rodríguez-Mirasol, J.A. Moulijn, J. Catal. 167 (1997) 256.
[18] J.N. Armor, Appl. Catal. B 1 (1992) 221.
[19] J.N. Armor, Micropor. Mesopor. Mater. 22 (1998) 451.
[20] R.M. Heck, Catal. Today 53 (1999) 519.
[21] H. Yahiro, M. Iwamoto, Appl. Catal. A 222 (2001) 163.
[22] B. Ganemi, E. Björnbom, J. Paul, Appl. Catal. B 17 (1998) 293.
[23] M. Iwamoto, H. Yahiro, K. Tanda, N. Mizuno, Y. Mine, S. Kagawa, J. Phys. Chem. 95 (1991) 3727.
[24] Y.J. Li, W.K. Hall, J. Phys. Chem. 94 (1990) 6145.
[25] M. Shelef, Catal. Lett. 15 (1992) 305.
[26] G. Spoto, A. Zecchina, S. Bordiga, G. Ricchiardi, G. Martra, G. Leofanti, G. Petrini, Appl. Catal. B 3 (1994) 151.
[27] S.K. Park, V. Kurshev, Z.H. Luan, C.W. Lee, L. Kevan, Micropor. Mesopor. Mater. 38 (2000) 255.
[28] S.C. Larsen, A. Aylor, A.T. Bell, J.A. Reimer, J. Phys. Chem. 98 (1994) 11533.
[29] A.T. Bell, Catal. Today 38 (1997) 151.
[30] A.W. Aylor, S.C. Larsen, J.A. Reimer, A.T. Bell, J. Catal. 157 (1995) 592.
[31] J. Dedecek, B. Wichterlová, Phys. Chem. Chem. Phys. 1 (1999) 629.
[32] D.J. Liu, H.J. Robota, Catal. Lett. 21 (1993) 291.
[33] M. Iwamoto, H. Yahiro, N. Mizuno, W.X. Zhang, Y. Mine, H. Furukawa, S. Kagawa, J. Phys. Chem. 96 (1992) 9360.
[34] Y.J. Li, W.K. Hall, J. Catal. 129 (1991) 202.
[35] J. Valyon, W.K. Hall, J. Phys. Chem. 97 (1993) 7054.
[36] B.L. Trout, A.K. Chakraborty, A.T. Bell, J. Phys. Chem. 100 (1996) 17582.
[37] W.F. Schneider, K.C. Hass, R. Ramprasad, J.B. Adams, J. Phys. Chem. B 102 (1998) 3692.
[38] B.R. Goodman, W.F. Schneider, K.C. Hass, J.B. Adams, Catal. Lett. 56 (1998) 183.
[39] G.D. Lei, B.J. Adelman, J. Sárkány, W.M.H. Sachtler, Appl. Catal. B 5 (1995) 245.
[40] Y. Teraoka, C. Tai, H. Ogawa, H. Furukawa, S. Kagawa, Appl. Catal. A 200 (2000) 167.
[41] P. Da Costa, B. Moden, G.D. Meitzner, D.K. Lee, E. Iglesia, Phys. Chem. Chem. Phys. 4 (2002) 4590.
[42] B.R. Goodman, K.C. Hass, W.F. Schneider, J.B. Adams, J. Phys. Chem. B 103 (1999) 10452.
[43] B. Moden, P. Da Costa, B. Fonfe, D.K. Lee, E. Iglesia, J. Catal. 209 (2002) 75.
[44] B. Moden, P. Da Costa, D.K. Lee, E. Iglesia, J. Phys. Chem. B 106 (2002) 9633.
[45] M.V. Konduru, S.S.C. Chuang, J. Catal. 196 (2000) 271.
[46] M.H. Groothaert, K. Pierloot, A. Delabie, R.A. Schoonheydt, Phys. Chem. Chem. Phys. 5 (2003) 2135.
[47] M.H. Groothaert, PhD thesis Nr. 534 at the Faculty of Agricultural and Applied Biological Sciences, K.U. Leuven, 2002.
[48] M.H. Groothaert, K. Lievens, J.A. van Bokhoven, A.A. Battiston, B.M. Weckhuysen, K. Pierloot, R.A. Schoonheydt, Chem. Phys. Chem. 4 (2003) 626.
[49] M.H. Groothaert, J.A. van Bokhoven, A.A. Battiston, B.M. Weckhuysen, R.A. Schoonheydt, J. Am. Chem. Soc. 125 (2003) 7629.
[50] L. Que, W.B. Tolman, Angew. Chem. Int. Ed. 41 (2002) 1114.
[51] J.A. Halfen, S. Mahapatra, E.C. Wilkinson, S. Kaderli, V.G. Young, L. Que, A.D. Zuberbühler, W.B. Tolman, Science 271 (1996) 1397.
[52] V. Mahadevan, M.J. Henson, E.I. Solomon, T.D.P. Stack, J. Am. Chem. Soc. 122 (2000) 10249.
[53] E.I. Solomon, M.D. Lowery, Science 259 (1993) 1575.
[54] I. Bertini, A. Sigel, H. Sigel, Handbook on Metalloproteins, Dekker, New York, 2001.

[55] B.M. Weckhuysen, Chem. Commun. (2002) 97.
[56] M. Iwamoto, H. Yahiro, Y. Mine, S. Kagawa, Chem. Lett. (1989) 213.
[57] R.L. Puurunen, B.G. Beheydt, B.M. Weckhuysen, J. Catal. 204 (2001) 253.
[58] H. Praliaud, S. Mikhailenko, Z. Chajar, M. Primet, Appl. Catal. B 16 (1998) 359.
[59] H. Yamashita, M. Matsuoka, K. Tsuji, Y. Shioya, M. Anpo, M. Che, J. Phys. Chem. 100 (1996) 397.
[60] Y. Itho, S. Nishiyama, S. Tsuruya, M. Masai, J. Phys. Chem. 98 (1994) 960.
[61] M. de Carvalho, F.B. Passos, M. Schmal, Appl. Catal. A 193 (2000) 265.
[62] G.T. Palomino, P. Fisicaro, S. Bordiga, A. Zecchina, E. Giamello, C. Lamberti, J. Phys. Chem. B 104 (2000) 4064.
[63] Y. Kuroda, R. Kumashiro, T. Yoshimoto, M. Nagao, Phys. Chem. Chem. Phys. 1 (1999) 649.
[64] I. Sanyal, M. Mahroof-Tahir, M.S. Nasir, P. Ghosh, B.I. Cohen, Y. Gultneh, R.W. Cruse, A. Farooq, K.D. Karlin, S. Liu, J. Zubieta, Inorg. Chem. 31 (1992) 4322.
[65] D. Sengupta, J.B. Adams, W.F. Schneider, K.C. Hass, Catal. Lett. 74 (2001) 193.
[66] M.V. Konduru, S.S.C. Chuang, X.H. Kang, J. Phys. Chem. B 105 (2001) 10918.
[67] E.I. Solomon, U.M. Sundaram, T.E. Machonkin, Chem. Rev. 96 (1996) 2563.